ELSEVIER

Chemical Engineering Journal 136 (2008) 373–382

Chemical Engineering Journal

www.elsevier.com/locate/cej

Theoretical analysis of the effect of catalyst mass distribution and operation parameters on the performance of a Pd-based membrane reactor for water–gas shift reaction

Giovanni Chiappetta [a], Gabriele Clarizia [a,*], Enrico Drioli [a,b]

[a] *Research Institute on Membrane Technology ITM-CNR, c/o University of Calabria via P. Bucci cubo 17/C, 87030 Arcavacata di Rende (CS), Italy*
[b] *Department of Chemical Engineering and Materials, University of Calabria, 87036 Arcavacata di Rende (CS), Italy*

Received 16 March 2007; received in revised form 8 May 2007; accepted 17 May 2007

Abstract

In the development of environmental friendly and highly efficient energy processes, membrane reactors hold an important role for their ability to carry out, simultaneously and in the same unit, the separation and reaction steps. Taking advantage of the synergies deriving from this coupling, they achieve comparable results to the conventional reactors at less severe conditions. A sensitivity analysis has been developed in order to define the role of some variables on the performance of a membrane reactor for maximizing the system efficiency. The behaviour of a membrane reactor has been investigated by means of a two-dimensional mathematical model applied to the water–gas shift reaction. By depending on operation feed pressure, a specific choice of both sweep gas flow rate and temperature can limit the occurring of dangerous temperature hot spots without compromising the performance of the system. The catalyst distribution coupled with an efficient heat exchange across the membrane have been investigated as possible technical solutions adequate to control hot spots along the membrane reactor.

Keywords: Non-isothermal membrane reactor; Axial and radial profiles; Catalyst mass distribution; Water–gas shift reaction

1. Introduction

The growing demand of energy in many industrial fields requires the conceiving of more efficient production and utilisation systems in a logic of sustainable development. Traditional energy systems (power plants or vehicles) are characterized by a low efficiency since over 60% of the input energy is lost; for this reason both new energy sources and more efficient devices would be explored. Hydrogen results an attractive energy carrier for its versatility in different refinery processes and applications as clean fuel [1].

Hydrogen is mainly produced from a variety of fossil fuels by either steam-hydrocarbon reforming or autothermal reforming for light feedstocks or partial oxidation using pure oxygen for heavy feedstocks, coal and coke [2]. In transport sector, the direct use of hydrogen is not widely distributed for still unsolved problems in the storage of gases, thus liquid fuels are considered for in situ hydrogen production by means of catalytic reforming processes. The presence of carbon monoxide in the reformate stream is a significant problem for a direct use in fuel cells since a few percentage of this gas poisons the catalyst. For this reason, additional steps to reduce CO content are required (*e.g.* methanation, selective oxidation, water–gas shift reaction). The water–gas shift reaction (WGSR)

$$CO + H_2O \Leftrightarrow H_2 + CO_2, \quad \Delta H_R = -40.6\,\mathrm{kJ\,mol^{-1}} \qquad (1)$$

represents a fundamental step in the main industrial routes to produce hydrogen [3] or for adjusting the CO/H_2 ratio of the syngas stream. High equilibrium conversion, no change in the total number of moles and moderate heat of reaction are the strong points of the WGSR investigated in this work. Furthermore, the stringent need to compact the space in vehicles imposes an efficient design of the fuel conversion units. In this framework membrane reactors (MRs), which are innovative devices capable to combine the separation and reaction steps in a single unit, can represent an interesting perspective. Smaller equipment volumes, lower energy losses, reduced control instrumentations are the main benefits of a correct merge of reaction and separation steps. A specific application of the MRs is the selective

* Corresponding author. Tel.: +39 0984 492037; fax: +39 0984 402103.
E-mail address: g.clarizia@itm.cnr.it (G. Clarizia).

1385-8947/$ – see front matter © 2007 Elsevier B.V. All rights reserved.
doi:10.1016/j.cej.2007.05.036

Nomenclature

a_k	constant
A_m	membrane area (m^2)
c_{H_2}	hydrogen concentration (kmol m^{-3})
c_i	concentration (kmol m^{-3})
$c_{i,0}$	feed concentration of the species i (kmol m^{-3})
c_{tot}	feed total concentration (kmol m^{-3})
Cp_{H_2}	hydrogen heat capacity (kJ kg^{-1} K^{-1})
Cp_{mix}	specific heat of the mixture on lumen side (kJ kg^{-1} K^{-1})
$Cp_{mix,shell}$	specific heat of the mixture on shell side (kJ kg^{-1} K^{-1})
d_p	diameter of catalyst pellet (m)
D	diameter of membrane tube (m)
$D_{i,r}$	radial effective diffusivity (m^2 s^{-1})
h_w	wall-heat transfer coefficient (kJ m^{-2} s^{-1} K^{-1})
J_{H_2}	hydrogen flow rate (kg m^{-2} s^{-1})
k_c	kinetic constant (atm^{-1} s^{-1})
L_r	catalyst bed length (m)
p_{feed}	total feed pressure (kPa)
$p_{H_2,lumen}$	hydrogen partial pressure (kPa)
$p_{H_2,shell}$	hydrogen partial pressure (kPa)
P_e	hydrogen permeance (kmol m^{-2} s^{-1} $Pa^{-0.5}$)
r	radial coordinate (m)
R	reactor radius (m)
R_{gas}	universal gas constant (cal mol^{-1} K^{-1})
$\Re_i$	reaction rate (kmol m^{-3} s^{-1})
T	temperature in the bed (K)
T_0	feed temperature (K)
$T_{0,shell}$	feed temperature on shell side (K)
T_w	wall temperature (K)
u_s	superficial velocity referred to whole section of lumen side (m s^{-1})
$u_{s,shell}$	superficial velocity referred to whole section of shell side (m s^{-1})
$v_z = u_s/\varepsilon$	interstitial fluid velocity in the axial direction (m s^{-1})
V_r	reactor volume (m^3)
y_i	molar fraction of the i-specie
z	axial coordinate (m)

Greek letters

ΔH	reaction enthalpy (kJ $kmol^{-1}$)
ε	bed voidage fraction
λ_{er}	effective radial thermal conductivity (kJ m^{-1} s^{-1} K^{-1})
$\rho_{g,shell}$, ρ_g	mixture density on shell and lumen sides (kg m^{-3})
ζ	dimensionless axial coordinate

Subscripts

0	at reactor inlet
B	catalytic bed
g	gas
i	compound
mix	mixture

removal of a product from the reaction ambient through the membrane by means of a partial pressure difference in order to enhance the conversion value shifting continuously the equilibrium [3]. Pd-based membranes, presenting selectivity values for hydrogen higher than other membrane materials and good mechanical and thermal stability, are particularly indicated in those reactions in which hydrogen is a product of the reaction [4]. The hydrogen pressure on retentate side should be sufficiently high in the whole membrane reactor to achieve the best performance of the unit. For this reason, technical solutions that allows to keep a constant and high hydrogen partial pressure value are particularly important for these devices.

Several authors developed mathematical models to predict the behaviour of membrane reactors. Most of these literature studies, involving the use of a MR as extractor, consider isothermal conditions and plug flow regime independently from the reaction type [5–13]. These models if applied to laboratory scale reactors are sufficiently accurate and they show higher conversion values than conventional reactors. However, by neglecting the thermal effects, they offer only a partial picture of the actual performance of the reactor in large scale applications. It was found that the isothermal assumption over-predicts the reactor performance and the degree of overestimation depends on the operating conditions [14]. Some authors investigated endothermic reactions in packed-bed membrane reactors still assuming plug flow in both feed and permeate sides but taking into account the heat effects [15–17], while other authors coupled exothermic and endothermic reactions without considering the dispersion term in the mass and energy balances [18].

In order to have a precise evaluation of inherent performance of a membrane reactor, some authors analysed the mass and heat transfer in the axial and radial directions applied to temperature distribution and hydrogen permeation for a highly endothermic reaction. The simulation results demonstrated that the temperature distribution in the reactor considerably changed in the axial and radial directions, and the hydrogen permeability through the membrane varied from position to position in the reactor [19]. On the other hand, few papers deal with exothermic reactions carried out in membrane reactors considering accurately both mass and energy balances [20].

For what concern the catalyst distribution, most of the theoretical and experimental studies were focused on the radial distribution of the active component in the catalyst pellets. Recently, some studies have revealed that an axially non-uniform catalyst distribution through the catalyst bed length may also affect considerably the process parameters [21]. It was shown that in the case involving first-order homogeneous and heterogeneous reactions in an isothermal reactor, the uniform distribution of the active component along the catalyst bed was optimal [22]. However, in order to mitigate the temperature gradients along the catalyst bed in an adiabatic catalytic reactor, an uniform distribution of the catalyst could not be necessarily optimal.

The use of side-streams and inert pellets to control the temperature profiles in addition to external cooling was developed and applied to laboratory-scale reaction systems by Hwang and Smith. The result of calculations performed on the nitrobenzene hydrogenation and ethylene oxidation in non-isothermal

and non-adiabatic reactors showed higher reactor performance in terms of conversion, yield or selectivity [23].

Aim of the present work is the analysis of the role of significant design parameters (sweep gas flow-rate and temperature, lumen pressure) on performance (conversion and hydrogen recovery) and hot spot control of a non-isothermal membrane reactor where the exothermic WGSR occurs. In addition, the effect of the catalyst distribution has been investigated.

2. Theoretical analysis

The behaviour of a MR has been investigated by means of a two-dimensional mathematical model. It considers, for heat and mass transport, the convective term in the axial direction and the diffusive term in the radial direction, neglecting the axial dispersion. These diffusive effects due to the conversion of the reagents have been neglected by selecting an appropriate ratio of catalyst bed length to particle size (L_r/d_p). The value calculated for this ratio is equal to 180; it meets the criterion concerning the minimum L_r/d_p ratio to limit significantly the axial dispersion in a reactor [24–26]. The radial convective flow is neglected because the membrane has a dense selective layer. In this way it is possible to simulate simultaneously the chemical reaction and the hydrogen separation through the membrane, taking into account both fluid dynamics and heat transfer inside the reactor. A sensitivity analysis has been developed in order to define the role of some variables on the performance of a membrane reactor for maximizing the system efficiency. The reagents are fed to the lumen of the tubular reactor in parallel mode with the sweep gas (steam) that, flowing in the shell side, extracts the product from the reaction zone through the Pd-based membrane. The membrane is completely selective for the hydrogen. All species involved in the process have been considered as ideal gases and for their physical properties (e.g. viscosity, density, specific heats, etc.) an average value as a function of temperature and composition has been assumed. A simplified scheme of the membrane reactor is shown in Fig. 1. The reaction system has been represented by a continuous single phase model (pseudo-homogeneous) which uses the effective transport concept to formulate the fluxes of heat and mass in the radial direction superimposed on the transport by overall convection (plug flow type). Therefore, the resulting two-dimensional differential equations, written in steady state for the lumen side

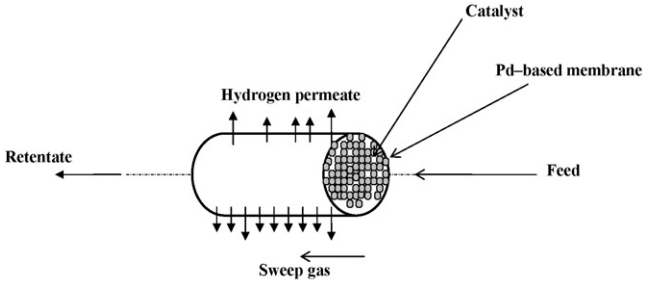

Fig. 1. Scheme of the tubular membrane reactor for water–gas shift reaction.

with the appropriate boundary conditions, are the following:

$$u_s \rho_g Cp_{mix} \frac{\partial T}{\partial z} = \frac{1}{r}\frac{\partial}{\partial r}\left(r\lambda_{er}\frac{\partial T}{\partial r}\right) + \Re_i(\Delta H(T)) \quad (2)$$

$$v_z \frac{\partial c_i}{\partial z} = \frac{1}{r}\frac{\partial}{\partial r}\left(rD_{i,r}\frac{\partial c_i}{\partial r}\right) + \Re_i \quad (3)$$

$$(B.C.1): \forall z,\ r = 0: \quad \frac{\partial c_i}{\partial r} = 0; \qquad \frac{\partial T}{\partial r} = 0$$

$$(B.C.2): \forall z,\ r = D/2$$

$$-D_{i,R}\frac{\partial c_i}{\partial r} = P_{H_2}\left(\sqrt{p_{H_2,lumen}} - \sqrt{p_{H_2,shell}}\right)$$

$$-\lambda_{er}\frac{\partial T}{\partial r} = h_w(T - T_w) + J_{H_2}Cp_{H_2}(T - T_w)$$

$$(B.C.3): \forall r,\ z = 0 \quad c_i = c_{i,0} \qquad T = T_0$$

As to boundary conditions, concentration and temperature gradients have been set equal to zero on the reactor axis (symmetry condition), while hydrogen diffusive flux at membrane surface is expressed by Sievert's law [27,28]. The temperature change in radial direction is the sum of the heat transferred across the metallic layer and the enthalpy associated with the hydrogen permeation. The concentration of the species and the temperature on both lumen and shell sides are known at the inlet of the MR. Heat and mass one-dimensional differential equations, written in steady state for the shell side, are the following:

$$u_{s,shell}\rho_{g,shell}Cp_{mix,shell}\frac{dT}{dz} = h_w(T_w - T) + J_{H_2}Cp_{H_2}(T_w - T) \quad (4)$$

$$u_{s,shell}\frac{dc_{H_2}}{dz} = \frac{A_m}{V_r}P_e\left(\sqrt{p_{H_2,lumen}} - \sqrt{p_{H_2,shell}}\right) \quad (5)$$

$$(B.C.4): z = 0 \quad T = T_{0,shell}$$

$$(B.C.5): z = 0 \quad c_{H_2} = 0$$

Eq. (4) considers that the temperature on the shell side can change also for effect of the sensible heat of the permeating hydrogen. This contribution is more significant as much as the permeating flow rate through the membrane increases. Hydrogen permeability obeys to Arrhenius' law with temperature. The sweep gas stream fed to the shell side of the MR does not contain hydrogen.

The partial differential equations have been discretised by means of an orthogonal collocation procedure at finite elements giving a set of ordinary differential equations solved by fourth order Runge–Kutta method. The collocation points, representative of mean compositions for each component and of the temperature in radial direction, have been determined by using a Legendre polynomial. The orthogonal collocation has already been applied to solve, in a reduced computation time also in fixed bed reactors, complex energy and mass balances, where non-linear terms are present [29].

Experimental values of membrane thickness and hydrogen permeation rates have been utilised in the computer code [30]. The Temkin's kinetic expression, considered for the water–gas shift reaction, is the following:

$$\Re_i = \frac{k_c p_{feed}(1-\varepsilon)c_{tot}\left((y_{CO}y_{H_2O}) - \left(\frac{(y_{H_2}y_{CO_2})}{K_{eq}}\right)\right)}{a_k y_{H_2O} + y_{CO_2}} \quad (6)$$

where $k_c = 6.0 \times 10^{11} \exp(-26{,}800/(R_{gas}T))$, $a_k = 2.5 \times 10^9 \exp(-21{,}500/(R_{gas}T))$ and $R_{gas} = 1.987$.

This expression was experimentally confirmed for a Cu–Zn–Cr low-temperature catalyst assuming an oxidation–reduction mechanism and no diffusive control for a grain size of 0.1–1 mm [31]. It fits better the experimental data in membrane reactors with respect to Langmuir–Hinshelwood model, as indicated in literature for isothermal conditions [32,33]. Preliminary experimental tests, carried out in non-isothermal conditions at 110 kPa, show the presence of a maximum in the temperature profile which can be explained by this kinetic model. In this work for the spherical pellets of catalyst, which are packed inside the tubular membrane, an unitary efficiency has been assumed (no internal and external transport resistance). The grain size of the catalyst does not affect the fluid dynamics of the system and the gas velocity in axial direction is independent on the radial position. The latter assumption is equivalent to neglect the pressure drops along the reactor due to the wall friction [29]. The catalytic bed depth has been assumed equal to the membrane length.

For practical purposes radial Peclet number has been assumed to lie between 8 and 10; from this dimensionless number the effective radial diffusion has been evaluated. In packed bed reactors, the effective heat conductivity, λ_{er}, decreases strongly close to the wall as a consequence of an additional resistance due to changes in the packing density and flow velocity. In this work, in order to describe the heat transfer in radial direction, a heat transfer coefficient at the wall, h_w, was introduced considering a constant value for λ_{er} in the reactor core, as suggested in literature [24,26].

In Table 1 are summarized the main parameters used in this work as base case. The effect of some parameter changes will be discussed in the next sections.

Table 1
Reference modelling parameters

Geometric and physical parameters	Value
Axial length of the catalyst bed (m)	0.15
Inside diameter of membrane (m)	0.01
Thickness of Pd/Ag film (m)	70×10^{-6}
Average particle diameter (m)	8.15×10^{-4}
Heat capacity of gas mixture in lumen side (kJ kg^{-1} K^{-1})	1.5
Heat capacity of gas mixture on shell side (kJ kg^{-1} K^{-1})	1.1
Hydrogen heat capacity (kJ kg^{-1} K^{-1})	14.5
Wall-heat transfer coefficient (kJ m^{-2} s^{-1} K^{-1})	1.6
Effective radial thermal conductivity (kJ m^{-1} s^{-1} K^{-1})	0.000297
Operating conditions	**Value**
Pressure on shell side (kPa)	110
Inlet feed temperature (K)	600
Limiting reagent flow rate (CO) (kmol min^{-1})	1.17×10^{-6}
Sweep gas flow-rate (kmol min^{-1})	1.17×10^{-5}
Feed molar ratio (H_2O/CO)	1

3. Results and discussion

3.1. Influence of the total feed pressure

As reported in literature, conventional reactors and hydrogen purification membranes at high pressures are used for water–gas shift reaction due to their compatibility with the gasifiers working at severe conditions of pressure and temperature, although this reaction is insensitive to pressure [34]. Consequently, in this work, the effect of the total feed pressure on the performance of a non-isothermal membrane reactor, where the WGSR takes place, has been investigated. Axial and radial temperature and concentration profiles have been analysed for three different pressure values (110, 500 and 2000 kPa). In the first part of the reactor, at each feed pressure value, it is possible to observe a temperature increase in the lumen side due to the heat produced by reaction not balanced by the heat released to the shell side, see Figs. 2–4. This net heat load available increases as feed pressure rises. In particular, at 500 kPa (Fig. 3) a significant temperature hot spot takes place close to the membrane reactor inlet. It results as a consequence of the quick evolution of the heat of reaction not balanced either by an efficient heat exchange towards the shell side (slow hydrogen permeation rate) or by a significant contribution of the endothermic reverse reaction.

As to the simulations performed at higher lumen pressures (e.g. 2000 kPa), differently from the previous case, they show a considerable reduction of the temperature hot spot intensity. As a consequence of the quick consumption of the reagents, the reverse reaction rate becoming more important lowers sharply the net forward rate and takes away heat from the reaction ambient. Furthermore, the high hydrogen partial pressure favouring the permeation towards shell side reduces the heat load removing sensible heat. In summary, the lumen temperature results lower than the previous case. At each pressure value, the more significant temperature variations occur on the reactor axis

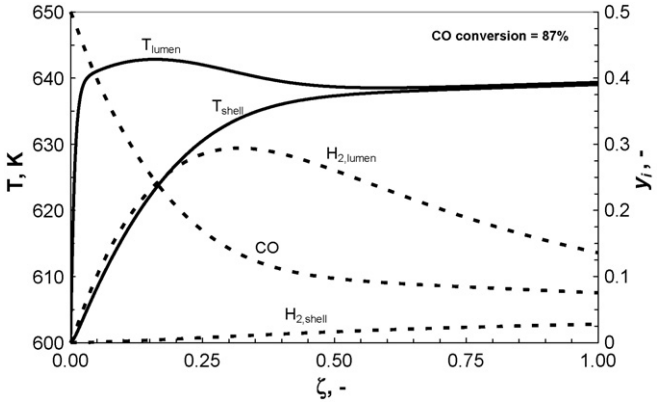

Fig. 2. Temperature (T, solid lines) and concentration (y_i, dotted lines) profiles along the reactor at a feed pressure equal to 110 kPa and inlet feed and shell temperatures of 600 K.

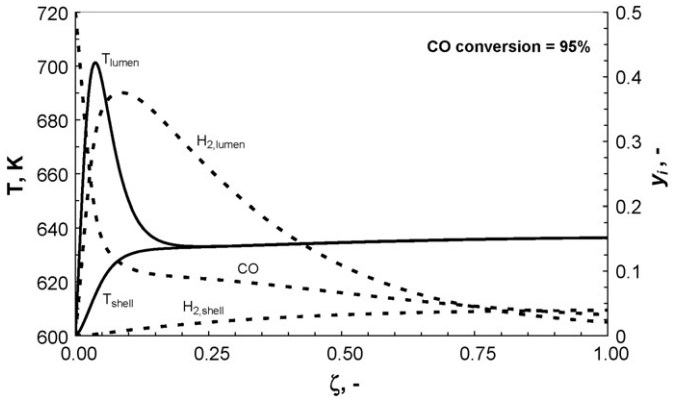

Fig. 3. Temperature (T, solid lines) and concentration (y_i, dotted lines) profiles along the reactor at a feed pressure equal to 500 kPa and inlet feed and shell temperatures of 600 K.

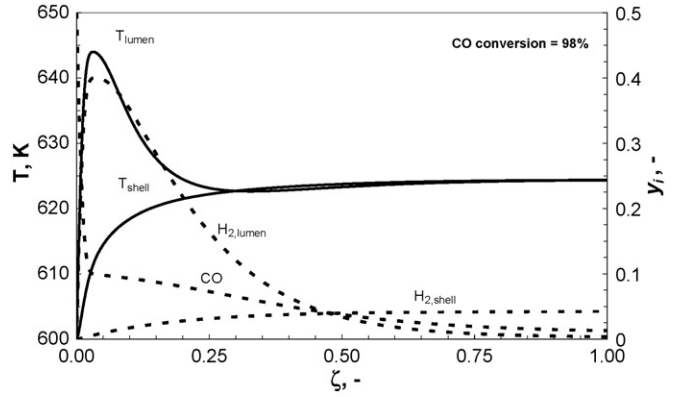

Fig. 4. Temperature (T, solid lines) and concentration (y_i, dotted lines) profiles along the reactor at a feed pressure equal to 2000 kPa and inlet feed and shell temperatures of 600 K.

and they tend to diminish shifting towards the reactor wall due to the cooling by the sweep gas, as shown in Figs. 5 and 6.

The increase of the feed pressure produces a high conversion of the reagents, available in a large amount, at distances closer to the membrane reactor inlet. As a consequence, the conversion

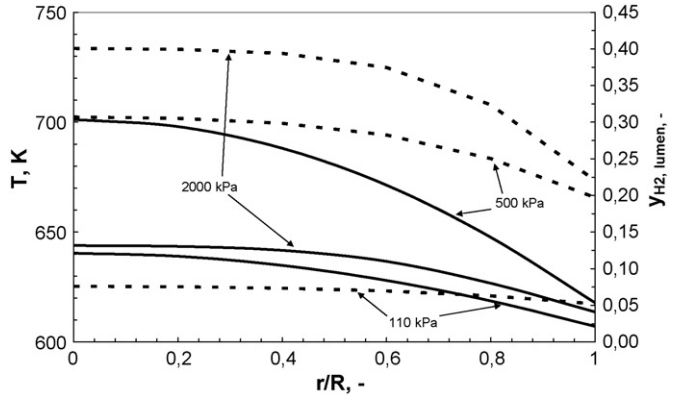

Fig. 5. Lumen temperature (T, solid lines) and hydrogen composition ($y_{H_2,lumen}$, dotted lines) vs. dimensionless radial position (at $\zeta = 0.04$, corresponding to the maximum temperature in the lumen side at 500 kPa) for three different feed pressure values.

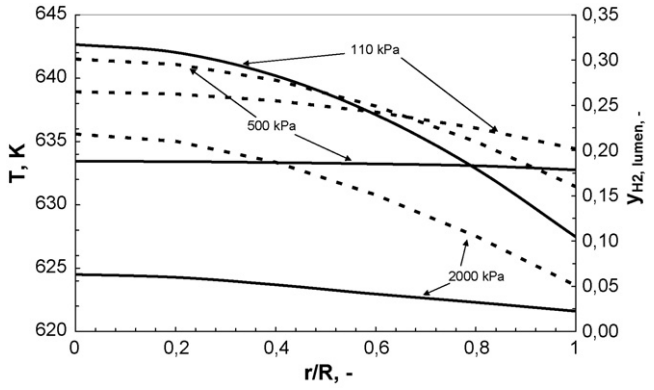

Fig. 6. Lumen temperature (T, solid lines) and hydrogen composition ($y_{H_2,lumen}$, dotted lines) vs. dimensionless radial position (at $\zeta = 0.2$) for three different feed pressure values.

increases gradually in the whole catalytic bed achieving a final value of 87% at 110 kPa, whereas it fast attains a plateau value for higher pressures (95 and 98% at 500 and 2000 kPa, respectively).

The presence of a peak for the hydrogen composition in the reaction zone depends on the balance between the hydrogen production and permeation rates. As the feed pressure increases, hydrogen generation rate increases as well; thus the peak occurs closer to the reactor inlet approaching a higher value (+37%) shifting from 110 to 2000 kPa. As a consequence of an enhanced hydrogen driving force along the membrane reactor, the final hydrogen content on the retentate side is reduced of the 97% shifting from 110 to 2000 kPa, while it increases on shell side of 50% (Figs. 2 and 4). Furthermore, the position of the peak of hydrogen concentration and the temperature hot spot coincides as the feed pressure value is high (2000 kPa); instead at lower feed pressures the two peaks are distinct and the maximum of temperature occurs before the hydrogen one depending on the different heat and mass transport rates.

Typically, a decrease in the efficiency of hydrogen separation occurs in a membrane reactor for effect of a decrease of the hydrogen flux through the membrane. It is due to a lowering of the hydrogen concentration in the radial direction (hydrogen partial pressure) close to the membrane interface during the permeation, as showed by Itoh et al. as two models based respectively on an ideal flow and radial diffusion are compared [35]. According to these observations, the temperature and hydrogen concentration profiles in the radial direction have been investigated at different feed pressure values and axial positions, see Figs. 5 and 6.

The parabolic shape of the temperature and hydrogen composition curves at each pressure for $\zeta = 0.04$ (Fig. 5) suggests that most of the resistance to the mass and heat transfer is close to the wall of the membrane and only a small amount is localised in the central core of the reactor. For what concerns the hydrogen composition, the higher feed pressure the higher hydrogen production (2000 kPa > 500 kPa > 110 kPa); however, the slow permeation rate of this product combined to its fast production rate at high feed pressures causes a radial concentration gradient that reduces, at 110 kPa, due to the slowest permeation and reaction rates.

At 500 kPa, the radial temperature gradients are more severe since the axial coordinate has been selected in correspondence of its maximum temperature. At 2000 kPa a flattening of the radial temperature profile in the central part, typical of a one-dimensional description, is produced because of the most of the conversion already takes place close to the inlet of the membrane reactor.

Fig. 6 shows lumen temperature and hydrogen composition radial profiles at $\zeta = 0.2$ where the effect of temperature hot spot is distant. At 110 kPa, a parabolic profile of temperature is still evident, due to a reduced heat exchange across the membrane. At higher pressure values, a flat temperature profile takes place since heat exchange results more efficient.

As a high hydrogen production rate is combined to a moderate permeation rate, a parabolic hydrogen composition profile is still observed (see Fig. 6 at 500 kPa). At 2000 kPa, in spite of the highest hydrogen production rate in the reactor, hydrogen content in the lumen side is lower due to the more significant role of the driving force on the hydrogen permeation with respect to 110 kPa, as discussed in depth for Figs. 2–4.

These results confirm that in a membrane reactor, for the water–gas shift reaction, the high pressure allows to combine both a higher recovery of hydrogen on shell side and a more efficient management of the heat transfer across the membrane.

3.2. Effect of the sweep gas

The sweep gas use in the membrane reactors is suggested since, enhancing the driving force, it increases the hydrogen permeating flow. In non-isothermal systems, it could favour also the heat exchange allowing a better control of the temperature in exothermic reactions. Therefore, the effect of sweep gas temperature and flow rate has been analysed in the following sections.

3.2.1. Inlet temperature

The influence of the sweep gas inlet temperature is represented in Figs. 7–10. If the inlet temperature on the shell side increases (500 K → 700 K) at the same feed pressure, the peak of lumen temperature for feed pressures lower than 2000 kPa rises as well due to a lower heat load transferred across the membrane towards the shell side. At $T_{shell} = 700$ K, the heat transferred by the sweep gas stream adds to the heat generated by the reaction, determining a fast temperature increase in the first part of the reactor ($\zeta < 0.05$). This trend results more significant at low feed pressures (110 kPa; Fig. 7), where the rate of forward reaction is accelerated by the heat entering from the shell side and not opposed by the occurring of the endothermic reverse reaction and hydrogen permeation (sensible heat removal). Thus, a temperature hot spot higher than that observed in Fig. 2, where $T_{shell} = T_{lumen} = 600$ K, arises. On the contrary, as the temperature on shell side is lower than the lumen side one, heat is continuously extracted by the sweep gas stream and the reaction and permeation rates are slowed down. This fact determines a lower hydrogen recovery on shell side (Fig. 10) combined with a higher hydrogen content in the lumen side (Fig. 9). On the other hand, as feed pressure

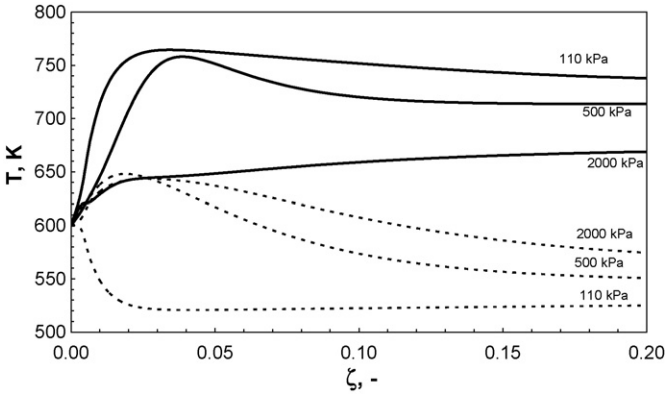

Fig. 7. Lumen temperature vs. dimensionless axial length as a function of feed pressure for two different sweep gas inlet temperature values (500 K, dotted lines) and (700 K, solid lines).

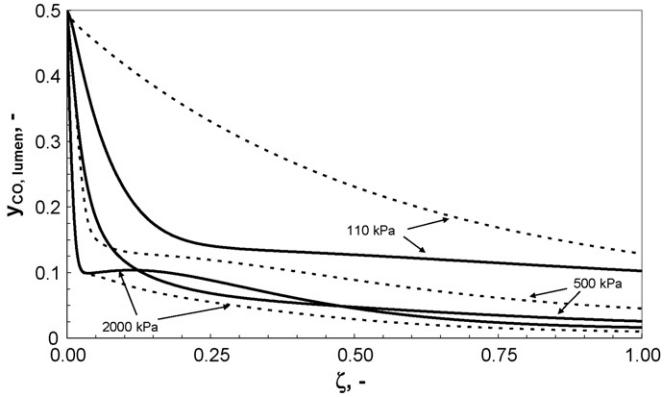

Fig. 8. CO lumen composition vs. dimensionless axial length as a function of feed pressure for two different sweep gas inlet temperature values (500 K, dotted lines) and (700 K, solid lines).

is high (2000 kPa), the effect of sweep gas temperature is not significant on the MR performance because hydrogen recovery, CO conversion and hydrogen content in lumen side are invariant with the investigated temperatures, see Figs. 8–10. At 2000 kPa, as $T_{shell} > T_{lumen}$ the consume of the reagents is still significantly higher than at lower pressures (Fig. 8). It

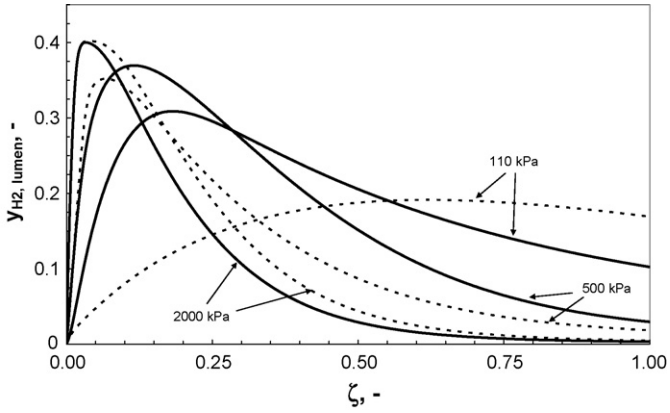

Fig. 9. H_2 lumen composition vs. dimensionless axial length as a function of feed pressure for two different sweep gas inlet temperature values (500 K, dotted lines) and (700 K, solid lines).

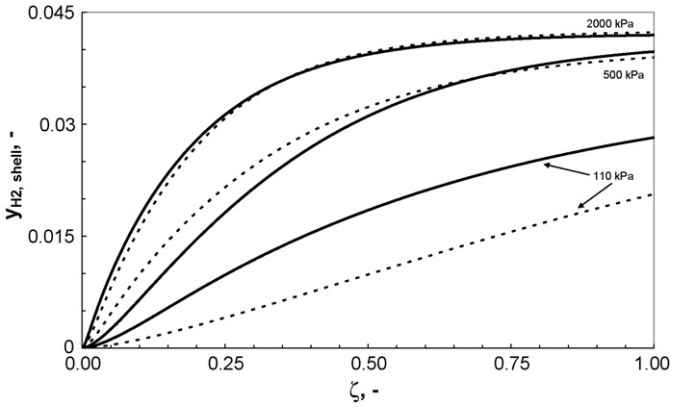

Fig. 10. H_2 shell composition vs. dimensionless axial length as a function of feed pressure for two different sweep gas inlet temperature values (500 K, dotted lines) and (700 K, solid lines).

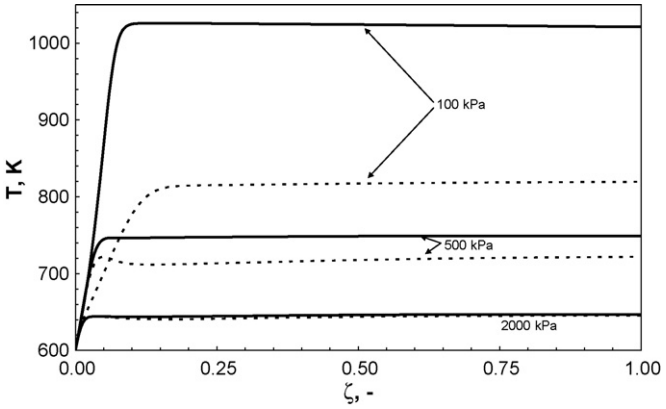

Fig. 11. Lumen temperature vs. dimensionless axial length as a function of feed pressure for two different sweep gas flow rates (0.00117 mol min^{-1}, dotted lines) and (0.000117 mol min^{-1}, solid lines).

favours the reverse reaction that, for its endothermic character, takes away quickly a part of reaction heat. As the hydrogen permeation towards the shell side becomes considerable, the forward reaction again prevails causing a progressive increase of the lumen temperature along the reactor as shown in Fig. 7. At feed pressure of 500 kPa, an intermediate behaviour with respect to the previous cases has been observed. As to the trend of hydrogen and CO composition profile, it is similar to that of 2000 kPa, whereas the temperature profile is closer to that of 110 kPa.

The temperature of the sweep gas does not affect the hydrogen concentration on shell side as the feed pressure is equal to 2000 kPa. The same trend is confirmed at 500 kPa, although the hydrogen amount results lower. At a feed pressure of 110 kPa, the value of $y_{H_2,shell}$, shell at the exit does not change at 600 and 700 K (Figs 2 and 10), whereas if T_{shell} is equal to 500 K, $y_{H_2,shell}$ results significantly lower (−27%) as shown in Fig. 10. In addition, the rate of increase of $y_{H_2,shell}$ depends on the T_{shell}.

These results put in evidence that at high feed pressures the influence of the sweep gas temperature on MR performance is not significant, while at a feed pressure equal to 110 kPa this variable becomes very important.

3.2.2. Inlet flow rate

Low sweep gas flow rates cause a significant increase of lumen temperature only at low feed pressure values (110 kPa). In fact, at this pressure value for $\zeta = 0.5$, as sweep gas flow rate decreases of an order of magnitude, the increase of lumen temperature is equal to 200 K (+25%), as shown in Fig. 11. In this case, the warming is due to a reduced cooling capability of the sweep gas stream; the heat of reaction, remaining inside the reactor, produces a generalised decrease of the global conversion value because of the endothermic reverse reaction is favoured. Thus, if the sweep gas flow rate becomes 100 times lower than reference value (0.0117 mol min^{-1}), the conversion changes from 87 to 54% with a CO content enhanced of three times. The hydrogen content in the lumen side results almost doubled.

As feed pressure increases, both the heat production and exchange rates rise determining a generalised decrease of the lumen temperature. Thus, at a sweep gas flow rate of 0.00117 mol min^{-1} moving from 110 to 2000 kPa the lumen temperature decreases of 170 K, while at 0.000117 mol min^{-1} it decreases of 370 K.

At 500 kPa, if the sweep gas flow rate is ten times lower, the lumen temperature increases of 30 K (Fig. 11) while a percentage decay of ten is observed for the conversion (86% → 76%). For what concerns the composition at the exit of membrane reactor, on lumen side, the CO content increases of two-thirds (Fig. 12), while the H_2 one becomes about three times higher (Fig. 13).

At feed pressure equal to 2000 kPa, the temperature profile is practically independent on sweep gas flow rate (Fig. 11). However, the conversion moves from 95 to 90% as the sweep gas flow rate decreases of 10 times, while the CO content doubles and H_2 concentration increases of about 300%.

On the basis of the results discussed above, at high feed pressure values (2000 kPa) the effect of sweep gas temperature and flow rate on the performance of the membrane reactor is less significant than at low feed pressure (110 kPa). However, at 2000 kPa is more convenient to operate with a sweep gas at a temperature (*e.g.* 500 K) lower than lumen temperature in terms of hydrogen recovery and CO conversion; nevertheless a low

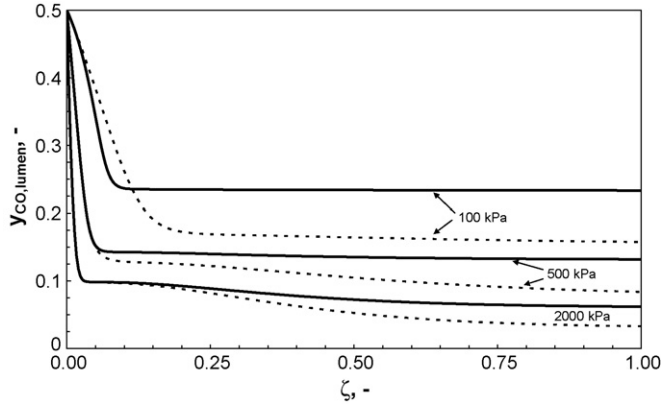

Fig. 12. CO lumen composition vs. dimensionless axial length as a function of feed pressure for two different sweep gas flow rates (0.00117 mol min^{-1}, dotted lines) and (0.000117 mol min^{-1}, solid lines).

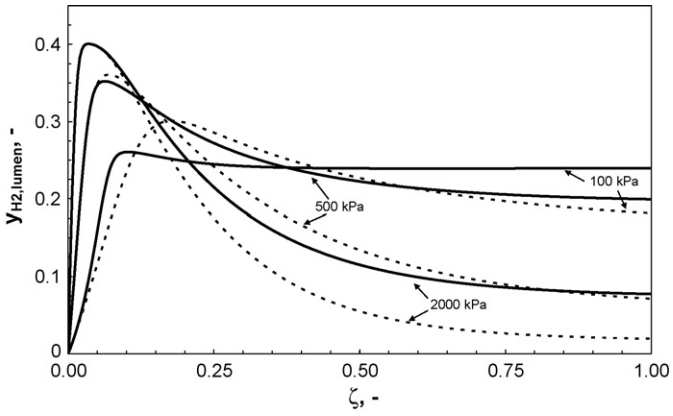

Fig. 13. H_2 lumen composition vs. dimensionless axial length as a function of feed pressure for two different sweep gas flow rates (0.00117 mol min^{-1}, dotted lines) and (0.000117 mol min^{-1}, solid lines).

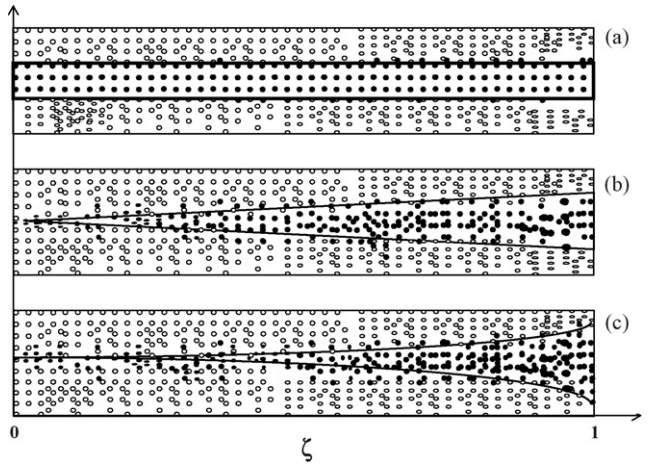

Fig. 14. Catalyst distributions along the membrane reactor: (a) constant, (b) linear, (c) exponential. Black circles represent the catalyst pellets, while white circles represent inert particles.

sweep gas flow rate favours a higher H_2 purity level without risk of an anomalous increase of lumen temperature. At 500 kPa is still opportune to work at $T_{shell} < T_{lumen}$ as to H_2 recovery and CO content in lumen side, while a low sweep gas flow rate is not advantageous as at 2000 kPa. On the contrary for a membrane reactor, at 110 kPa it is absolutely not recommended to operate at low sweep gas flow rate, while a sweep gas temperature at least equal to lumen temperature is suggested in order to achieve high CO conversion and H_2 recovery on shell side.

3.3. Effect of the catalyst mass distribution

Another mode to control the intensity of temperature hot spot and use efficiently a membrane reactor is to operate on the catalyst distribution. This method could be an alternative to the use of side-streams and inert pellets to control the temperature profiles in addition to an external intermediate cooling applied successfully also to laboratory scale reaction systems by Hwang and Smith [23].

As previous discussed in Section 3.1, close to the membrane reactor entry, an excess of heat is generated by the high conversion value of the fresh reagents. In the rest of the unit, at high feed pressures, a reduced increase of the conversion has been observed. Therefore, the opportunity to dose the catalyst along the membrane reactor has been considered by setting a lower catalyst mass where the hot spot occurs and a higher catalyst amount in the zone where the increase of the conversion is negligible. As a consequence, two different catalyst distributions (linear and exponential) have been investigated in addition to the constant mode described previously. A qualitative picture of all catalyst distribution modes is reported in Fig. 14. The results, in terms of temperature and hydrogen concentration profiles, on both lumen and shell sides, have been compared with those discussed in the previous sections for a constant catalyst allotment.

The simulations, in Fig. 15, show how a catalyst mass that increases linearly along the membrane reactor produces a temperature hot spot less significant with respect to an exponential distribution. At 2000 kPa, the effect of the feed pressure on the temperature profile is preponderant with respect to the catalyst distribution. In fact, the hot spot intensity does not change while only the outlet temperature in the lumen side results slightly lower as a linear distribution is considered. On the contrary, at 500 kPa an influence of the catalyst distribution is observed since the temperature hot spot is reduced: 700 K for constant, 687 K for exponential and 672 K for linear modes, respectively. As to the outlet temperatures, the lowest value (623 K) is still for the linear while the highest one (650 K) is for the exponential mode.

At 110 kPa, a linear distribution lowers further both the hot spot intensity and outlet temperature (625 K) with respect to the value for the constant mode (643 K). An exponential distribution generates a progressive increment of the temperature in the whole catalytic bed. In this case, the combination of a large amount of the reagents still unconverted and catalyst in the second half of the reactor produces an uncontrolled warming of the unit with a consequent decrease of the conversion. The conversion value at 110 kPa changes from 87 to 59% moving from a linear to an exponential allocation. This behaviour confirms the fundamental role of the linear distribution at low feed pressure values.

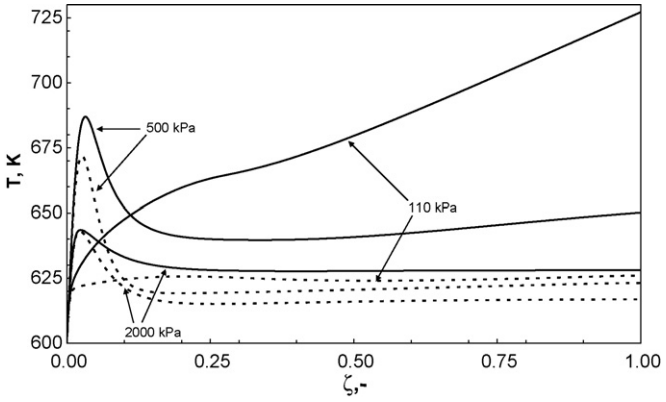

Fig. 15. Lumen temperature vs. dimensionless axial length as a function of feed pressure for two different catalyst distributions: linear (dotted lines) and exponential (solid lines).

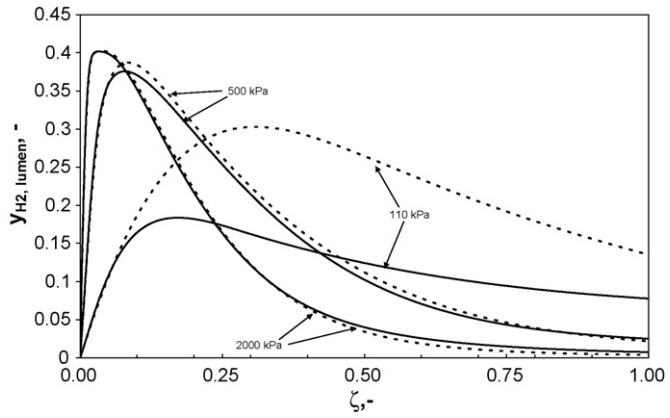

Fig. 16. H_2 lumen composition vs. dimensionless axial length as a function of feed pressure for two different catalyst distributions: linear (dotted lines) and exponential (solid lines).

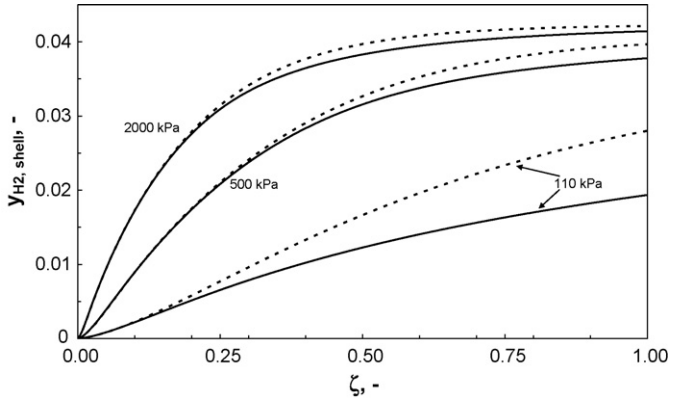

Fig. 17. H_2 shell composition vs. dimensionless axial length as a function of feed pressure for two different catalyst distributions: linear (dotted lines) and exponential (solid lines).

For what concerns the hydrogen concentration, similar profiles are observed for all catalyst distributions independently on the feed pressure (Figs. 16 and 17). However, if at high pressures (2000 kPa) the advantage of a linear catalyst distribution is moderated, it becomes progressively more significant at 500 and 110 kPa with respect to an exponential distribution.

4. Conclusions

A theoretical analysis for the complete understanding of the behaviour of a membrane reactor, where an exothermic reaction occurs, has to take into account both mass and heat transport phenomena. By means of this approach it is possible to combine opportunely the operation and design parameters for achieving high conversion and recovery values. An appropriate choice of the feed pressure, sweep gas flow rate and temperature has a beneficial effect on the driving force for hydrogen permeation, conversion and temperature profile, mitigating eventual dangerous hot spots or avoiding thermal runaway. For the same aim, the opportunity to dose the catalyst along the membrane reactor has been established by setting a lower catalyst mass where the reaction rate is important and a higher catalyst amount in the zone where the increase of the conversion is less significant. At high feed pressures, the influence of the sweep gas temperature and flow rate on the performance of the membrane reactor is less remarkable than at low feed pressure. At 2000 kPa, it is more convenient to operate with a sweep gas at lower temperature (e.g. 500 K) than lumen temperature in terms of hydrogen recovery and CO conversion; nevertheless a low sweep gas flow rate favours a higher H_2 purity level, without risk of an anomalous increase of lumen temperature. On the other hand, at 110 kPa it is strongly suggested to use a large sweep gas flow rate at the same temperature of the feed stream in order to achieve high CO conversion and H_2 recovery. A catalyst mass that increases linearly along the membrane reactor is more efficient than an exponential distribution to control the temperature hot spots. However, if at high pressures (2000 kPa) the advantage of a linear catalyst distribution is moderated, it becomes progressively more significant at 500 and 110 kPa with respect to an exponential distribution.

The advantages of all solutions illustrated in this study could be further enhanced in presence of more permeable and equally selective materials used as membranes.

References

[1] K.P. De Jong, H.M.H. Van Wechem, Carbon: hydrogen carrier or disappearing skeleton? Int. J. Hydrogen Energy 20 (6) (1995) 493–499.
[2] M. Conte, A. Iacobazzi, M. Ronchetti, R. Vellone, Hydrogen economy for a sustainable development: state-of-the-art and technological perspectives, J. Power Sources 100 (2001) 171–187.
[3] G. Saracco, H.W.J.P. Neomagus, G.F. Versteeg, W.P.M. van Swaaij, High temperature membrane reactors: potential and problems, Chem. Eng. Sci. 54 (13–14) (1999) 1997–2017.
[4] R. Dittmeyer, V. Hollein, K. Daub, Membrane reactors for hydrogenation and dehydrogenation processes based on supported palladium, J. Mol. Catal. A: Chem. 173 (2001) 135–184.
[5] S. Uemiya, N. Sato, H. Ando, E. Kikuchi, The water–gas shift reaction assisted by a palladium membrane reactor, Ind. Eng. Chem. Res. 30 (1991) 585–589.
[6] J. Galuszka, R.N. Pandey, S. Ahmed, Methane conversion to syngas in a palladium membrane reactor, Catal. Today 46 (1998) 83–89.
[7] J. Zaman, A. Chakma, A simulation study on the thermal decomposition of hydrogen sulfide in a membrane reactor, Int. J. Hydrogen Energy 20 (1) (1995) 21–28.
[8] J.M. Sousa, A. Mendes, Modeling a dense polymeric catalytic membrane reactor with plug flow pattern, Catal. Today 82 (2003) 241–254.
[9] J.M. Sousa, A. Mendes, Modelling a catalytic membrane reactor with plug flow pattern and a hypothetical equilibrium gas-phase reaction with $\Delta n \neq 0$, Catal. Today 104 (2005) 336–343.
[10] J.N. Keuler, L. Lorenzen, The dehydrogenation of 2-butanol in a Pd–Ag membrane reactor, J. Membr. Sci. 202 (2002) 17–26.
[11] O.P. Radovan, G.M. Ciric, M.N. Tekic, R.N. Paunovic, Applicability of two-membrane reactors for reversible gas phase reaction. Effects of flow patterns and inerts, J. Membr. Sci. 128 (1997) 213–221.
[12] D. Chmielewski, Z. Ziaka, V. Manousiouthakis, Conversion targets for plug flow membrane reactors, Chem. Eng. Sci. 54 (1999) 2979–2984.
[13] W. Liang, R. Hughes, The catalytic dehydrogenation of isobutane to isobutene in a palladium/silver composite membrane reactor, Catal. Today 104 (2–4) (2005) 238–243.
[14] W. Yu, T. Ohmori, T. Yamamoto, A. Endo, M. Nakaiwa, T. Hayakawa, N. Itoh, Simulation of a porous ceramic membrane reactor for hydrogen production, Int. J. Hydrogen Energy 30 (10) (2005) 1071–1079.
[15] R.P. Omorjan, R.N. Paunovic, M.N. Tekic, Non-isothermal two-membrane reactors for reversible gas phase reactions, J. Membr. Sci. 138 (1998) 57–66.

[16] A. Kleinert, G. Grubert, X. Pan, C. Hamel, A. Seidel-Morgenstern, J. Caro, Compatibility of hydrogen transfer via Pd-membranes with the rates of heterogeneously catalysed steam reforming, Catal. Today 104 (2005) 267–273.
[17] J. Huang, L. El-Azzami, W.S.W. Ho, Modeling of CO_2-selective water–gas shift membrane reactor for fuell cell, J. Membr. Sci. 261 (2005) 67–75.
[18] N. Itoh, W. Tian-Hua, An adiabatic type of palladium membrane reactor for coupling endothermic and exothermic reactions, J. Membr. Sci. 124 (2) (1997) 213–222.
[19] C. Fukuhara, A. Igarashi, Two-dimensional simulation of a membrane reactor for dehydrogenation of ethylbenzene, considering heat and mass transfer, J. Chem. Eng. Jpn. 36 (5) (2003) 530–539.
[20] T.P. Tiemersma, C.S. Patil, M. van Sint Annaland, J.A.M. Kuipers, Modelling of packed membrane reactors for autothermal production of ultrapure hydrogen, Chem. Eng. Sci. 61 (2006) 1602–1616.
[21] V.M. Khanaev, E.S. Borisova, A.S. Noskov, Optimization of the active component distribution through the catalyst bed for the case of adiabatic reactor, Chem. Eng. Sci. 60 (2005) 5792–5802.
[22] S. Melis, A. Varma, C.J. Pereira, Optimal distribution of catalyst for a case involving heterogeneous and homogeneous reactions, Chem. Eng. Sci. 52 (2) (1997) 165–169.
[23] S. Hwang, R. Smith, Heterogeneous catalytic reactor design with optimum temperature profile. I. Application of catalyst dilution and side-stream distribution, Chem. Eng. Sci. 59 (2004) 4229–4243.
[24] G.F. Froment, K.B. Bischoff, Chemical Reactor Analysis and Design, second ed., John Wiley, New York, 1990.
[25] D.E. Mears, The role of axial dispersion in trickle-flow laboratory reactor, Chem. Eng. Sci. 26 (1971) 1361.
[26] P. Andrigo, R. Bagatin, G. Pagani, Fixed bed reactors, Catal. Today 52 (1999) 197–221.
[27] F.A. Lewis, The Palladium Hydrogen System, Academic Press, London, 1967.
[28] J. Shu, B.P.A. Grandjean, A. Van Neste, S. Kaliaguine, Catalytic palladium-based membrane reactors: a review, Can. J. Chem. Eng. 69 (Oct. 1991).
[29] E. Gobina, K. Hou, R. Hughes, Ethane dehydrogenation in a catalytic membrane reactor coupled with a reactive sweep gas, Chem. Eng. Sci. 50 (14) (1995) 2311–2319.
[30] S. Tosti, A. Basile, G. Chiappetta, C. Rizzello, V. Violante, Pd–Ag membrane reactors for water–gas shift reaction, Chem. Eng. J. 93 (2003) 23–30.
[31] D.S. Newsome, P. Kellog, The water–gas shift reaction, Catal. Rev. Sci. Eng. 21 (2) (1980) 275–318.
[32] A. Criscuoli, A. Basile, E. Drioli, An analysis of the performance of membrane reactors for the water–gas shift reaction using gas feed mixtures, Catal. Today 56 (2000) 53–64.
[33] A. Basile, G. Chiappetta, S. Tosti, V. Violante, Experimental and simulation of both Pd and Pd/Ag for a water–gas shift membrane reactor, Sep. Purif. Technol. 25 (2001) 549–571.
[34] M.V. Mundschau, X. Xie, C.R. Evenson, A.F. Sammells, Membranes for the purification of hydrogen produced from coal-derived water–gas shift mixtures, in: Proceedings of the 22nd Annual International Pittsburgh Coal Conference, 2005, pp. 12/1–12/8.
[35] N. Itoh, W.C. Xu, K. Haraya, Radial mixing diffusion of hydrogen in a packed-bed type of palladium membrane reactor, Ind. Eng. Chem. Res. 33 (22) (1994) 197–220.